Optical Squeezing in Temporal, Polarization and Spatial Domains

T. Symul[a], W. P. Bowen[a], R. Schnabel[a], N. Treps[a,b], B. C. Buchler[a], T. C. Ralph[c], A. M. Lance[a], N. B. Grosse[a], A. Dolińska[a], J. W. Wu[a], J. R. Gao[a], C. Fabre[b], H. -A. Bachor[a] and P. K. Lam[a,*]

[a]Quantum Optics Group, Department of Physics, The Australian National University, Canberra ACT 0200, Australia.

[b]Laboratoire Kastler Brossel, Université Pierre et Marie Curie, case 74, 75252 Paris cedex 05, France.

[c] Department of Physics, Centre for Quantum Computer Technology, University of Queensland, St Lucia, QLD 4072 Australia.

ABSTRACT

We present methods of transforming the standard quadrature amplitude squeezing of a continuous-wave light beam to its Stokes parameters and transverse spatial modes statistics. These two states of light are called *polarization squeezing* and *spatial squeezing*, respectively. We present experimental results of the quadrature amplitude, polarization and spatial squeezing obtained with a common experimental setup based on optical parametric amplifiers. The transformations from quadrature amplitude to polarization and spatial squeezing are achieved with only simple linear optics.

Keywords: squeezed light, spatial squeezing, polarization squeezing, optical parametric amplifier.

1. INTRODUCTION

Given a set of non-commuting variables, the Heisenberg principle imposes uncertainty limits on the simultaneous measurements of these variables. For example, if $[A, B] = \delta$ we would obtain the Heisenberg uncertainty relation of $\Delta^2 A \Delta^2 B \geq \delta^2/4$, where $\Delta^2 O = \langle O^2 \rangle - \langle O \rangle^2$ is the variance of the measurement of an observable O. For the last two decades, squeezed light has been used to circumvent quantum measurement noise by making the pair of uncertainty variances of the two non-commuting variables asymmetric. The observable of interest, say A, can then be determined to an accuracy greater than the standard quantum limit at the expense of the other observable B, with $\Delta^2 A < |\delta/2| < \Delta^2 B$.

The first and many subsequent demonstrations of squeezing[1] were performed on the quadrature amplitudes of light. A beam of light can be either amplitude or phase squeezed. In this paper, we refer to this form of squeezing as *temporal squeezing* since the light statistics of both amplitude and phase squeezing are temporally ordered. Temporal squeezing is proposed to be used in many applications, ranging from improvements of interferometric sensitivity[2] to the demonstration of quantum teleportation.[3,4] Recently, there has been increasing interest in the utilization of temporal squeezing in large scale gravitational wave detectors.[5] In Section 2, we present our experimental results of quadrature amplitude squeezing.

The Stokes parameters of a light beam which define its polarization state can also be squeezed. Polarization squeezing is interesting because it has the potential to couple the quantum states of light to atomic ensembles.[6] In some quantum information protocols, polarization squeezing can be used to facilitate communication without the need of a network wide universal local oscillator.[7] The commutation relations of Stokes parameters are discussed in Section 3 and the squeezing results are presented using the Poincaré representation.

* Further correspondence to P.K.L.: E-mail: Ping.Lam@anu.edu.au, Telephone: +61 (0)2 6125 2747, Telefax: +61 (0)2 6125 0741.

Fluctuations and Noise in Photonics and Quantum Optics, Derek Abbott, Jeffrey H. Shapiro, Yoshihisa Yamamoto, Editors, Proceedings of SPIE Vol. 5111 (2003) © 2003 SPIE · 0277-786X/03/$15.00

More recently, it has also been demonstrated that different parts of the transverse spatial profile of a light beam can exhibit quantum correlations. This form of spatial ordering is referred to as *spatial squeezing*. Spatial squeezing has applications in situations where the displacement, or the pointing direction, of a laser beam needs to be determined with great accuracy. For example, displacement measurements of atomic force microscope cantilever may ultimately be limited by the quantum noise of its optical readout beam. We present the basic method and experimental results for generating one dimensional spatially squeezed light in Section 4.

Since optical squeezing is now the basic resource for generating optical entanglement, we briefly discuss how the three forms of squeezed light can potentially be useful in quantum information protocols, such as quantum cryptography and quantum imaging in Section 5.

2. TEMPORAL SQUEEZING

2.1. Theory

The Heisenberg uncertainty principle when applied to an optical field gives the relation

$$\Delta X^+ \Delta X^- \geq 1 \tag{1}$$

where $X^+ = \hat{a} + \hat{a}^\dagger$, and $X^- = -i(\hat{a} - \hat{a}^\dagger)$, are respectively the amplitude and phase quadratures of the light mode described by the annihilation operator $\hat{a}$. Two kind of minimum uncertainty states can be discerned : the coherent states for which both amplitude and phase quadrature variances are equal to 1, and the squeezed states for which one quadrature variance falls below 1. In the following we will use the linearized operators assumption[8] where the annihilation operator is written as $\hat{a} = \alpha + \delta\hat{a}$. α and $\delta\hat{a}$ denote the steady state component and the zero mean value fluctuations of the annihilation operator, respectively.

An optical parametric amplifier (OPA) below threshold can produce squeezed states of light. Assuming that the OPA is a simple Fabry-Perot cavity with a second order non-linear gain medium inside, the equation of motion of the OPA in the non-pump depletion regime is given by[9]

$$\dot{a} = g\hat{a}^\dagger - \kappa\hat{a} + \sqrt{2\kappa_b}\hat{A}_b + \sqrt{2\kappa_f}\hat{A}_f + \sqrt{2\kappa_l}\delta\hat{A}_l \tag{2}$$

where $\hat{A}_f$ and $\hat{A}_b$ are the input fields injected into the front and back mirrors and $\delta\hat{A}_l$ is a vacuum fluctuation term due to loss in the cavity. $\kappa = \kappa_f + \kappa_b + \kappa_l$ is the total cavity damping rate, where κ_f, κ_b and κ_l are the damping rates of the front and back mirrors and the loss in the cavity, respectively. The parameter g takes into account the second order non-linear interaction and is proportional to the second harmonic pump field.

The output from the OPA expressed in terms of an input $\hat{A}_f$ can be derived from Eq. (2). In the ideal limit, no vacuum fluctuation couples into the cavity. This can be modelled by setting $\kappa_b = 0$ and $\kappa_l = 0$. The output field quadratures from the OPA expressed in the frequency domain are

$$X^+_{\text{out}}(\omega) = \frac{\kappa_f - i\omega + g}{i\omega + \kappa - g} X^+_f(\omega) \tag{3}$$

$$X^-_{\text{out}}(\omega) = \frac{\kappa_f - i\omega - g}{i\omega + \kappa + g} X^-_f(\omega) \tag{4}$$

where the general operator $Z = Z(\omega)$ is the Fourier transform of the time operator $\hat{Z} = \hat{Z}(t)$. By assuming the detection frequency is small compare with the cavity linewidth, such that $\omega \ll \kappa$, the output field quadratures can be expressed more succinctly as

$$X^+_{\text{out}} = \sqrt{G} X^+_f \tag{5}$$

$$X^-_{\text{out}} = \frac{1}{\sqrt{G}} X^-_f \tag{6}$$

where the parametric gain is defined as $G = [(\kappa_f + g)/(\kappa_f - g)]^2$. The amount of gain is dependent on the pump power, and on the relative phase between the pump and input beams. In the amplification regime phase squeezed light is produced, whilst in the deamplification regime amplitude squeezed light is produced.

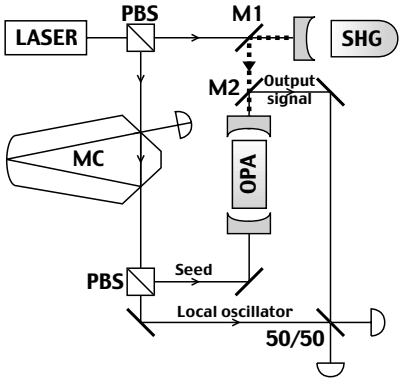

Figure 1. Schematic for generating squeezed light with an OPA. SHG: Second harmonic generator, OPA: optical parametric amplifier, MC: Mode cleaner cavity, PBS: polarizing beam splitter, M1,M2: Dichroic mirrors, 50/50: symmetric beam splitter.

2.2. Experimental setup

The basic experimental setup used to generate temporal squeezing is depicted Fig. 1. The laser is a non-planar ring diode-pumped continuous wave Nd:YAG laser, generating a TEM_{00} beam at 1064 nm. The Second Harmonic Generator (SHG) is a hemilithic cavity consisting of a MgO:$LiNbO_3$ nonlinear crystal with an input planar surface anti-reflection coated and a spherical back surface high-reflection coated, both for 1064 nm and 532 nm. The green light at 532 nm produced by the SHG is sent to the OPA using a dichroic mirror, M1. The mode cleaner cavity is a high finesse ring cavity which is used to filter frequency noise above its cavity bandwidth. The transmitted beam, which is quantum noise limited at the detection frequency, is used as a seed for the OPA and as a local oscillator for the characterization of the squeezed light.

The OPA is either a monolithic cavity based on a single $MgO:LiNbO_3$ nonlinear crystal for experiments requiring only one squeezer, or a hemilithic cavity similar to the SHG cavity for the experiments requiring two squeezed sources. The advantages of the monolithic cavity are that it is very stable and has very low losses, resulting in a large amount of squeezing. The advantage of the hemilithic cavity is that it is easier to be servo controlled. The quadrature angle of the squeezing (relative to the seed beam) is chosen by locking the relative phase of the pump beam to either a maximum or minimum of the output power from the OPA cavity. The minimum corresponds to amplitude quadrature squeezing, while the maximum gives phase quadrature squeezing. The output beam of the OPA is spatially separated with a dichroic mirror.

The temporally squeezed beam was analyzed with an optical homodyne setup. This is done by mixing the output beam with the local oscillator on a 50/50 beam splitter and the resulting beams were detected using two high quantum efficiency EPITAXX ETX-500 photodiodes. The difference of the photocurrents produced by these detectors, which can be either sent directly to a spectrum analyzer, or demodulated at a particular frequency and recorded on an oscilloscope, describes a particular quadrature of the output state depending on the relative phase, θ_{LO}, between the output beam and the local oscillator.

2.3. Results

At a pump power of around $60\% \pm 10\%$ of the OPA threshold, the best amplitude quadrature squeezing was experimentally observed.[10] Using a monolithic OPA cavity, we obtained 7.0 ± 0.2 dB of vacuum squeezing at a detection frequency of 3 MHz. Experimental reconstruction of the Wigner function of the vacuum state and squeezed vacuum state were also performed with this setup using optical homodyne tomography.[11] The reconstructed Wigner function of the squeezed vacuum state produced by the monolithic OPA, see Fig. 2 (a), exhibits 4.1 dB of squeezing, and 8.7 dB of anti-squeezing. The lower value of the squeezing is due to the optical homodyne tomography method which requires much more data points than a direct homodyne measurement, thus introducing an averaging effect. Fig. 2 (b) shows a coherent vacuum state used as a calibration of the experiment.

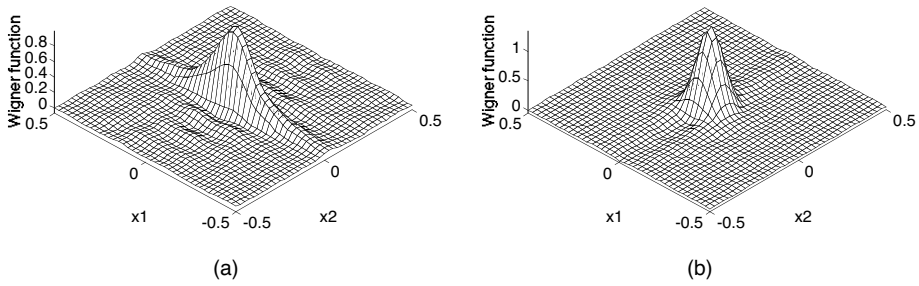

Figure 2. Experimental Wigner function plots of (a) a squeezed vacuum state and, (b) a coherent vacuum state.

With the hemilithic cavities, the best measured amplitude quadrature squeezing[12] was 4.5 dB at 6.5 MHz. This smaller squeezing value was due to additional losses on the extra surfaces inside the OPA resonator. Using hemilithic OPA cavities, however, enabled us to simultaneously keep more than one OPA locked on resonance. We can therefore generate two temporally squeezed beams with 2 OPAs. This is useful for generating polarization squeezing or 2D spatial squeezing as we will see in Sections 3 and 4.

3. POLARIZATION SQUEEZING

3.1. Theory

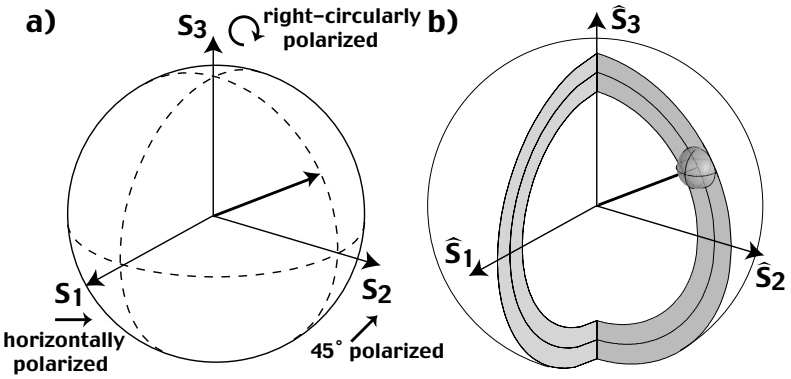

Figure 3. a) classical and b) quantum Stokes vectors mapped on a Poincaré sphere; the ball at the end of the quantum vector visualizes the quantum noise in $\hat{S}_1$, $\hat{S}_2$, and $\hat{S}_3$; and the non-zero quantum sphere thickness visualizes the quantum noise in $\hat{S}_0$.

The polarization state of a light beam in classical optics can be visualized as a Stokes vector on a Poincaré sphere (Fig. 3) and is determined by the four Stokes parameters: S_0 represents the beam intensity whereas S_1, S_2, and S_3 characterize its polarization and form a cartesian axes system. If the Stokes vector points in the direction of S_1, S_2, or S_3 the polarized part of the beam is horizontally, linearly at 45°, or right-circularly polarized, respectively. Two beams are said to be opposite in polarization and do not interfere if their Stokes vectors point in opposite directions. The quantity $S = (S_1^2 + S_2^2 + S_3^2)^{1/2}$ is the radius of the classical Poincaré sphere and the fraction S/S_0 $(0 < S/S_0 < 1)$ is called the *degree of polarization*. For quasi-monochromatic laser light which is almost completely polarized S_0 is a redundant parameter, completely determined by the other three parameters ($S_0 = S$ in classical optics). The quantum-mechanical analogue of the classical Stokes parameters for

pure states[13] in the commonly used notation are defined as:

$$\begin{aligned} \hat{S}_0 &= \hat{a}_H^\dagger \hat{a}_H + \hat{a}_V^\dagger \hat{a}_V \ , \quad \hat{S}_2 = \hat{a}_H^\dagger \hat{a}_V + \hat{a}_V^\dagger \hat{a}_H, \\ \hat{S}_1 &= \hat{a}_H^\dagger \hat{a}_H - \hat{a}_V^\dagger \hat{a}_V \ , \quad \hat{S}_3 = i\hat{a}_V^\dagger \hat{a}_H - i\hat{a}_H^\dagger \hat{a}_V, \end{aligned} \tag{7}$$

where the subscripts H and V label the horizontal and vertical polarization modes respectively, and the $\hat{a}_{H,V}$ and $\hat{a}_{H,V}^\dagger$ are annihilation and creation operators for the light field in frequency domain. The commutation relations of the annihilation and creation operators

$$[\hat{a}_k, \hat{a}_l^\dagger] = \delta_{kl} \ , \quad \text{with} \quad k,l \in \{H,V\} \ , \tag{8}$$

directly result in Stokes operator commutation relations,

$$[\hat{S}_1, \hat{S}_2] = 2i\hat{S}_3 \ , \ \ [\hat{S}_2, \hat{S}_3] = 2i\hat{S}_1 \ , \ \ [\hat{S}_3, \hat{S}_1] = 2i\hat{S}_2 \ . \tag{9}$$

Apart from a normalization factor, these relations are identical to the commutation relations of the Pauli spin matrices. In fact the three Stokes parameters in Eq. (9) and the three Pauli spin matrices both generate the special unitary group of symmetry transformations SU(2) of Lie algebra. Since this group obeys the same algebra as the three-dimensional rotation group, distances in three dimensions are invariant. Accordingly the operator $\hat{S}_0$ is also invariant and commutes with the other three Stokes operators ($[\hat{S}_0, \hat{S}_j] = 0$, with $j = 1,2,3$). It can be shown from Eqs. (7) and (8) that the quantum Poincaré sphere radius is different from its classical analogue, $\left\langle \hat{S} \right\rangle = \left\langle \hat{S}_0^2 + 2\hat{S}_0 \right\rangle^{1/2}$. This is another consequence of the quantum noise in the Stokes parameters. On the other hand quantum states of partial and opposite polarization can be defined in direct analogy to the classical description. The noncommutability of the Stokes operators $\hat{S}_1$, $\hat{S}_2$ and $\hat{S}_3$ precludes the simultaneous exact measurement of their physical quantities. As a direct consequence of Eq.(9) the Stokes operator mean values $\left\langle \hat{S}_j \right\rangle$ and their variances $V_j = \left\langle \hat{S}_j^2 \right\rangle - \left\langle \hat{S}_j \right\rangle^2$ are restricted by the uncertainty relations

$$V_1 V_2 \geq |\left\langle \hat{S}_3 \right\rangle|^2 \ , \ V_2 V_3 \geq |\left\langle \hat{S}_1 \right\rangle|^2 \ , \ V_3 V_1 \geq |\left\langle \hat{S}_2 \right\rangle|^2 \ . \tag{10}$$

In general this results in non-zero variances in the individual Stokes parameters as well as in the radius of the Poincaré sphere (see Fig. 3b).[13]

To calculate the Stokes operator variances we again use the linearized formalism. The creation and annihilation operators are expressed as sums of complex classical amplitudes $\tilde{\alpha}_{H,V}$ and quantum noise operators $\delta\hat{a}_{H,V}$:

$$\hat{a}_{H,V} = \tilde{\alpha}_{H,V} + \delta\hat{a}_{H,V} \quad \text{and} \quad \tilde{\alpha}_{H,V} = \alpha_{H,V} e^{i\theta_{H,V}}. \tag{11}$$

where we have introduced the modulus and the phase of the complex amplitudes. The operators in Eq. (11) are non-hermitian and therefore unphysical. To express the Stokes operators of Eq. (7) in terms of hermitian operators we define the generalized quadrature quantum noise operators $\delta\hat{X}_{H,V}(\phi)$, rotating them such as they point into the phase and amplitude direction :

$$\delta\hat{X}_{H,V}(\phi) = \delta\hat{a}_{H,V}^\dagger e^{i(\phi+\theta_{H,V})} + \delta\hat{a}_{H,V} e^{-i(\phi+\theta_{H,V})}, \tag{12}$$

$$\delta\hat{X}_{H,V}^+ = \delta\hat{X}_{H,V}(\phi{=}0), \tag{13}$$

$$\delta\hat{X}_{H,V}^- = \delta\hat{X}_{H,V}(\phi{=}\pi/2). \tag{14}$$

ϕ is the phase of the quantum mechanical oscillator and $\delta\hat{X}_{H,V}^+$ and $\delta\hat{X}_{H,V}^-$ are the amplitude quadrature noise operator and the phase quadrature noise operator respectively.

If the variances of the noise operators are much smaller than the coherent amplitudes then a first order approximation of the noise operators is appropriate. This yields the Stokes operator mean values

$$\begin{aligned} \left\langle \hat{S}_0 \right\rangle &= \alpha_H^2 + \alpha_V^2 = \langle \hat{n} \rangle \ , \ \left\langle \hat{S}_2 \right\rangle = 2\alpha_H \alpha_V \cos\theta \ , \\ \left\langle \hat{S}_1 \right\rangle &= \alpha_H^2 - \alpha_V^2 \ , \qquad \left\langle \hat{S}_3 \right\rangle = 2\alpha_H \alpha_V \sin\theta \ , \end{aligned} \tag{15}$$

Where we have introduced the relative phase between the two beams as $\theta = \theta_V - \theta_H$. These expressions are identical to the Stokes parameters in classical optics. Here $\langle \hat{n} \rangle$ is the expectation value of the photon number operator. For a coherent beam the expectation value and variance of $\hat{n}$ have the same magnitude, this magnitude equals the conventional shot-noise level. The variances of the Stokes parameters are given by

$$\begin{aligned} V_0 &= \alpha_H^2 \left\langle (\delta \hat{X}_H^+)^2 \right\rangle + \alpha_V^2 \left\langle (\delta \hat{X}_V^+)^2 \right\rangle + 2\alpha_H \alpha_V \left\langle \delta \hat{X}_H^+ \delta \hat{X}_V^+ \right\rangle , \\ V_1 &= \alpha_H^2 \left\langle (\delta \hat{X}_H^+)^2 \right\rangle + \alpha_V^2 \left\langle (\delta \hat{X}_V^+)^2 \right\rangle - 2\alpha_H \alpha_V \left\langle \delta \hat{X}_H^+ \delta \hat{X}_V^+ \right\rangle , \\ V_2(\theta) &= \alpha_H^2 \left\langle (\delta \hat{X}_V(-\theta))^2 \right\rangle + \alpha_V^2 \left\langle (\delta \hat{X}_H(\theta))^2 \right\rangle + 2\alpha_H \alpha_V \left\langle \delta \hat{X}_V(-\theta) \delta \hat{X}_H(\theta) \right\rangle , \\ V_3(\theta) &= V_2(\theta - \frac{\pi}{2}) . \end{aligned} \tag{16}$$

It can be seen from Eqs.(16) that the variances of Stokes operators can be expressed in terms of the variances of quadrature operators of two modes. Polarization squeezing can then be defined in a straight forward manner. The variances of the noise operators in the above equation are normalized to one for a coherent beam. Therefore the variances of the Stokes parameters of a coherent beam are all equal to the shot-noise of the beam. For this reason a Stokes parameter is said to be squeezed if its variance falls below the shot-noise of an equal power coherent beam. Although the decomposition to the H, V-polarization axis of Eqs. (16) is independent of the actual procedure of generating a polarization squeezed beam, it becomes clear that two overlapped quadrature squeezed beams can produce a single polarization squeezed beam. If two beams in the horizontal and vertical polarization mode having uncorrelated quantum noise Eqs. (16) can be rewritten as

$$\begin{aligned} V_0 = V_1 &= \alpha_H^2 \left\langle (\delta \hat{X}_H^+)^2 \right\rangle + \alpha_V^2 \left\langle (\delta \hat{X}_V^+)^2 \right\rangle , \\ V_2(\theta) &= \cos^2\theta \left(\alpha_V^2 \left\langle (\delta \hat{X}_H^+)^2 \right\rangle + \alpha_H^2 \left\langle (\delta \hat{X}_V^+)^2 \right\rangle \right) + \sin^2\theta \left(\alpha_V^2 \left\langle (\delta \hat{X}_H^-)^2 \right\rangle + \alpha_H^2 \left\langle (\delta \hat{X}_V^-)^2 \right\rangle \right) , \\ V_3(\theta) &= V_2(\theta - \frac{\pi}{2}) . \end{aligned} \tag{17}$$

It can be seen from Eq.(17) that for polarization squeezing generated from two amplitude squeezed beams, the $\hat{S}_0$ and two additional Stokes parameters can in theory be perfectly squeezed when $\theta = 0$ or $\theta = \pi/2$ are used. Utilizing only one temporally squeezed beam, it is not possible to simultaneously squeeze any two of $\hat{S}_1$, $\hat{S}_2$, and $\hat{S}_3$ to more than 3 dB below the standard quantum limit.

3.2. Experimental setup

The experimental setup used to generate polarization squeezing[14,15] is depicted Fig. 4 (A). The refractive index of the MgO:$LiNbO_3$ crystal in each OPA resonator was modulated with an RF field, this provided error signals on the reflected and transmitted seed power that were used to lock their length. The modulation also resulted in a phase modulation on the output beams from the SHG and each OPA. The coherent amplitude of each OPAs output was a deamplified/amplified version of the seed coherent amplitude; the level of amplification was dependent on the phase difference between pump and seed (ϕ_{sh}). Therefore the second harmonic pump phase modulation resulted in a modulation of the amplification of the OPAs, error signals could be extracted from this effect, enabling the relative phase between pump and seed to be locked. Locking to deamplification or amplification provided an amplitude or phase squeezed output, respectively.

Instanstaneous values of the Stokes operators of all polarization states analyzed in this paper were obtained with the the apparatus shown in Fig. 4 (B). The beam under interrogation was split on a polarizing beam splitter and the two outputs were detected on a pair of high quantum efficiency photodiodes with 30 MHz bandwidth; the resulting photocurrents were added and subtracted to yield photocurrents containing the instantaneous values of $\hat{S}_0$ and $\hat{S}_1$. To measure $\hat{S}_2$ the polarization of the beam was rotated by 45° with a half-wave plate before the polarizing beam splitter and the detected photocurrents were subtracted. To measure $\hat{S}_3$ the polarization of the beam was again rotated by 45° with a half-wave plate and a quarter-wave plate was introduced before the polarizing beam splitter such that a horizontally polarized input beam became right-circular. Again the detected

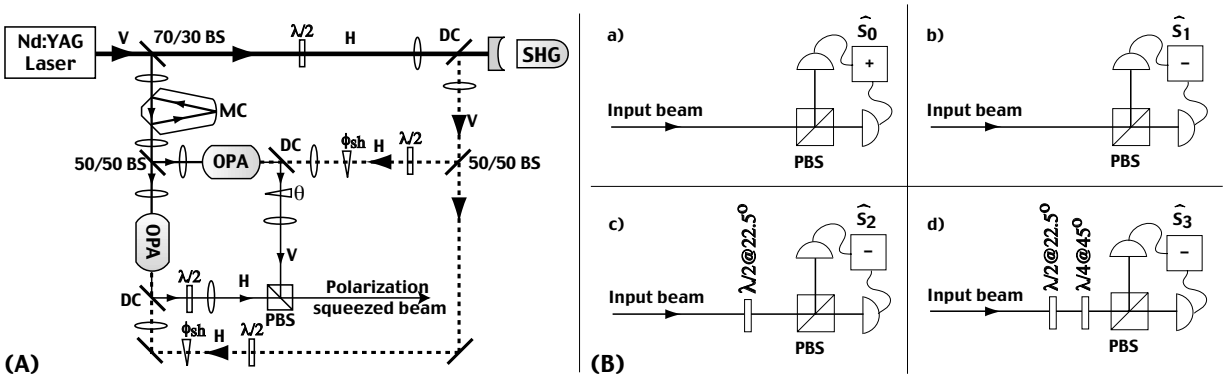

Figure 4. (A) Schematic of the polarization squeezing experiment and (B) apparatus required to measure each of the Stokes parameters. DC: dichroic beam splitter, $\lambda/2$ and $\lambda/4$: half- and quarter-wave plates respectively ϕ_{sh}: phase shift between 532 nm and 1064 nm light at the OPAs, θ: phase shift between quadrature squeezed beams, H: horizontal polarization mode, V: vertical polarization mode.

photocurrents were subtracted. The expectation value of each Stokes operator was equal to the DC output of the detection device and the variance was obtained by passing the output photocurrent into a Hewlett-Packard E4405B spectrum analyzer.

3.3. Results

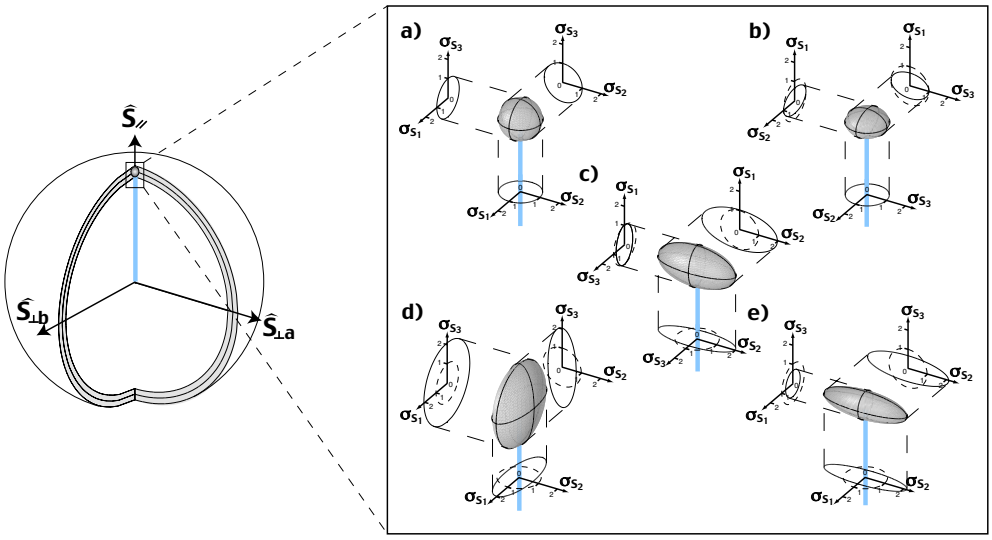

Figure 5. Measured quantum polarization noise at 8.5 MHz from different combinations of two input beams: a) coherent beam and vacuum, b) bright squeezed beam and vacuum, c) coherent beam and squeezed vacuum, d) two amplitude squeezed beams and e) two phase squeezed beams. The surface of the ellipsoids defines the standard deviation of the noise normalized to shot-noise ($\sigma_{S_i} = \sqrt{V_i}$).

Four different kinds of polarization squeezing were realized as depicted Fig. 5. We first characterized the polarization state of a single horizontally polarized bright amplitude squeezed beam provided by one of the OPAs. The Stokes operators $\hat{S}_0$ and $\hat{S}_1$ were squeezed respectively 3.2 dB and 3.6 dB below the shot noise at 8.5 MHz, while the variances of the remaining Stokes operators $\hat{S}_2$ and $\hat{S}_3$ were at the shot noise level (see Fig. 5 b). Then we mixed a bright horizontally polarized coherent beam with a dim vertically polarized amplitude

squeezed beam. The variances of $\hat{S}_0$ and $\hat{S}_1$ where slightly above the shot noise level, while $\hat{S}_2$ was anti-squeezed and $\hat{S}_3$ squeezed 2.8 dB below the shot noise at 8.5 MHz (see Fig. 5.c). For the third experiment, we mixed two phase squeezed beams respectively horizontally and vertically polarized. $\hat{S}_0$, $\hat{S}!_1$ and $\hat{S}_3$ were all anti-squeezed, and $\hat{S}_2$ was squeezed optimally 2.8 dB below the shot noise at 4.8 MHz (see Fig. 5.c). Finally, we mixed two amplitude squeezed beams respectively horizontally and vertically polarized. $\hat{S}_0$, $\hat{S}_1$ and $\hat{S}_3$ were all below the shot noise with respective maximum squeezing of 3.8 dB at 9.3 MHz, 4.3 dB at 5.7 MHz and 3.5 dB at 9.3 MHz, while the remaining stokes operator $\hat{S}_2$ was anti squeezed (see Fig. 5.e).

4. SPATIAL SQUEEZING

4.1. Theory

Precision optical imaging using CCD cameras or photodetector arrays is required in many areas of science, ranging from astronomy to biology. Ultimately, the performance of optical imaging technology is limited by quantum mechanical effects. Of particular importance, as far as applications are concerned, is the measurement of image displacements, for example, the position of a laser beam. Techniques that rely on determining the position of a laser spot include atomic force microscopy, measurement of very small absorption coefficients via the mirage effect and observation of the motion of single molecules. These measurements are usually performed using a laser beam centered on a split detector that delivers two currents proportional to the light intensity integrated over the two halves ($x < 0$ and $x > 0$) of the image plane. If the beam is initially centered on the detector, the mean value of the photocurrent difference is directly proportional to the relative displacement d of the beam with respect to the detector. With a classical, shot noise limited laser source, the smallest displacement that can be measured (with a signal-to-noise ratio of one) is shown to be[16]

$$d_{\mathrm{SQL}} = \frac{\sqrt{N}}{2I(0)}. \tag{18}$$

Here N is the total number of photons recorded by the two detectors during the measurement time, and $I(0)$ is the local density of photons (photons per unit transverse length) at the position of the boundary between the two detectors. For a TEM_{00} Gaussian beam with radius w_0, the minimum measurable displacement is found to be

$$d_{\mathrm{SQL}} = \sqrt{\frac{\pi}{8}}\frac{w_0}{\sqrt{N}}. \tag{19}$$

For maximum focusing of the Gaussian beam, $w_0 = \lambda$, and we obtain $d_{\mathrm{SQL}} \approx \lambda/\sqrt{N}$, which is the absolute minimum displacement of a physical system that can be measured with classical beams. Equation (19) shows that a more powerful laser, or a longer measurement time, gives increased measurement precision. However, in many applications these alternatives are simply not practical. In the case of atomic force microscopy, for example, excessive laser power ultimately leads to radiation pressure noise. For biological applications, large laser power may damage the samples under investigation and an increased integration time leads to loss of bandwidth. This is the motivation for looking for alternative methods of increasing measurement precision.

The limit of equation (19) can be surpassed only using multimode non-classical light. Let us consider a beam of light with an electric field distribution given by $E(x)$. We can build an orthonormal basis of the transverse plane $\{u_i\}$ such that $u_0 = E(x)/\parallel E(x) \parallel$ is the first vector; u_1 is a "flipped" mode, given by $-u_0(x)$ for $x < 0$ and $u_0(x)$ for $x > 0$; and the other modes are choosen in order to form a basis. In this basis, the mean field of our light lies only in the first mode u_0 but, a priori, all of the modes contribute to the quantum noise. In order to determine the relevant modes of our measurement, we consider the interference quantities between two modes on each half of the split detector:

$$\begin{aligned} I_{x<0}(u_i, u_j) &= \int_{-\infty}^{0} u_i^*(x)u_j(x)dx \\ I_{x>0}(u_i, u_j) &= \int_{0}^{+\infty} u_i^*(x)u_j(x)dx. \end{aligned} \tag{20}$$

Then the interference quantities relevant for a total measurement (sum of the two photodetectors) and a differential measurement (difference of the two photodetectors) can be written:

$$\begin{aligned} I_{\text{sum}}(u_i u_j) &= I_{x<0}(u_i, u_j) + I_{x>0}(u_i, u_j) \\ I_{\text{diff}}(u_i u_j) &= I_{x<0}(u_i, u_j) - I_{x>0}(u_i, u_j) \end{aligned} \tag{21}$$

One can then show that for any transverse mode u_i,

$$I_{\text{sum}}(u_i u_1) = I_{\text{diff}}(u_i u_0). \tag{22}$$

Since all u_i, for $i \geq 2$, are orthonormal to u_1 (i.e. $I_{\text{sum}}(u_i u_1) = 0$), equation (22) demonstrates that these modes have a zero overlap integral with u_0 in a differential measurement. It can then be shown that only u_1, which has a non-zero overlap integral with u_0, has to be considered along with u_0 in the noise calculation.[16]

We note that the modes u_0 and u_1 have perfect interference visibility as shown by their complete overlap integral for the differential measurement, ie. $I_{\text{diff}}(u_0 u_1) = 1$. In this regard, the measurement is analogous to a perfect homodyne measurement with a beam splitter. The two modes are equivalent to the two input beams of a beamsplitter and the two halves of the multimode beam are equivalent to the two outputs. Therefore, similar to a homodyne measurement, the noise on the differential measurement is completely cancelled when the flipped mode is occupied by a perfect squeezed vacuum, with the squeezed quadrature in phase with the coherent field of the $u_0(x)$ mode.

4.2. Experimental setup

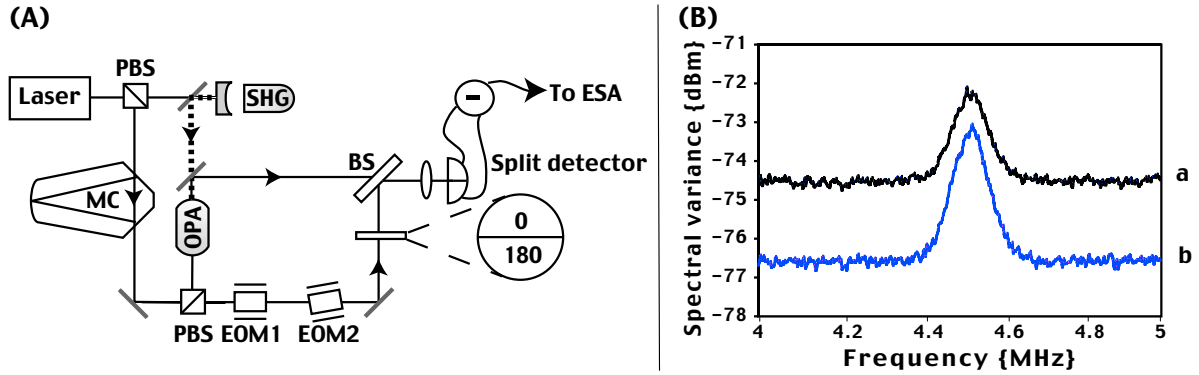

Figure 6. (A) Scheme of the experimental setup and (B) experimental results. (A) EOM: Electro-Optic Modulator and ESA: Electronic Spectrum Analyzer. The dashed lined correspond to light at 532 nm and the solid line to the light at 1064 nm. The TEM00 mode is produced by the OPA and is a squeezed vacuum, the flipped mode is a coherent state. (B) Noise spectrum of the photocurrent difference in presence of an oscillating displacement with amplitude 2.9 Åat a frequency of 4.5 MHz (resolution bandwidth: 100 kHz) a) using a coherent state of light and, b) using the spatially squeezed light. These traces were obtained by averaging the signal over 10 successive traces.

The experimental setup for generating spatial squeezing[17] is shown in Fig. 6 (A). The flipped mode, $u_1(x)$, is produced by sending the remaining part of the initial 1064 nm laser beam through a specially designed phase plate. This phase plate consists of two birefringent half-wave plates, one rotated by 90° with respect to the other, forming the two halves $x < 0$ and $x > 0$ of the transverse plane. These elements introduce a phase shift of 180° between the field amplitudes of the two halves. The squeezed output from the OPA is required to be superimposed onto the flipped mode with minimal loss. This is achieved by using a beam splitter that reflects 92% of the squeezed state and transmits 8% of the coherent state. The reflected output is then sent to a quadrant InGaAs detector (EPITAXX 505Q) with quantum efficiency greater than 90%. A lens is used to image the phase plate on the detector plane and to counteract the diffraction of the flipped mode, which undergoes an abrupt phase change and therefore contains high spatial frequency components. In order to produce a small controllable

beam displacement in the frequency range of the previous measurements, we use two electro-optic modulators (EOMs) driven at 4.5 MHz. Fig. 6 (A) shows that EOM2 is slightly tilted with respect to the propagation of the light beam. When a voltage is applied across EOM2, a change in refractive index is induced and the transmitted beam experiences a parallel transverse displacement measured at about 3nm/V. Apart from the parallel displacement, EOM2 will also introduce an unwanted phase modulation on the transmitted beam which is detrimental to our measurement. EOM1 of Fig. 6 (A) is therefore used to compensate for this introduced phase modulation. When correct gains are chosen for both modulators, the transmitted beam will not have any phase or amplitude modulation and are only left with pure transverse displacement modulation.

4.3. Results

Figure 6 (B) shows the differential signal monitored by a spectrum analyzer when the light beam undergoes a displacement modulation with an amplitude of 2.9Å. Fig. 6 (B)a shows the trace when vacuum instead of the squeezed vacuum is used in mode $u_0(x)$. Thus this noise floor gives the standard quantum limit in such a displacement measurement. The signal-to-noise ratio (SNR) of this measurement is 0.68. When the two-mode non-classical beam is utilized in the measurement (Fig. 6 (B)b), we obtain a SNR of 1.20. This gives an improvement of the displacement measurement sensitivity by a factor of 1.7. The result is in agreement with the theoretical value calculated with the noise reduction reported in the previous paragraph.

5. DISCUSSION AND CONCLUSIONS

Of the three forms of continuous variable squeezing introduced in the previous sections, we point out that only temporal squeezing has realized some of its application potential for quantum information. Whilst further work is still needed to extend the utility of polarization and spatial squeezing.

In principle experimental demonstrations of polarization squeezing[6, 14, 18] and entanglement[19] have been performed. Polarization entanglement, however, is more diverse in the sense that entanglement may exist between some or all combinations of the pairs of the Stokes parameters. To date, full entanglement of all Stokes parameters has not been experimentally demonstrated in the continuous variable regime.

Transfer of optical polarization quantum states to atomic spin ensembles has been experimentally demonstrated.[6] There is therefore, potential for polarization entanglement to be transferred to spatially distant pairs of atomic ensembles, which is a crucial element in most proposed quantum information networks.

Our work on spatial squeezing has demonstrated that a one-dimensional displacement measurement can have accuracy surpassing the standard quantum limit. More complex arrangements of non-classical beams can be used to extend spatial squeezing to two dimensions, or even to detection on arrays of pixels. Since quadrature amplitude entanglement can be generated from temporal squeezing, one can explore the possibility of generating spatial entanglement from spatial squeezing. The combination of the multi-pixel extension and the possibility of generating spatial entanglement is an enabling step towards parallel processing of quantum information via the transmission of quantum images.

ACKNOWLEDGMENTS

We thank the Australian Research Council for financial support. RS is supported by the Alexander von Humboldt foundation. This project is part of EU QIPC Project, No. IST-1999-13071 (QUICOV).

REFERENCES

1. R. E. Slusher, L. W. Hollberg, B. Yurke, J. C. Mertz, and J. F. Valley, "Observation of squeezed states generated by four-wave mixing in an optical cavity," *Phys. Rev. Lett.* **55**, p. 2409, 1985.
2. M. Xiao, L. Wu, and H. J. Kimble, "Precision measurement beyond the shot-noise limit," *Phys. Rev. Lett.* **59**, p. 278, 1987.
3. A. Furusawa, J. L. Sorensen, S. L. Braunstein, C. A. Fuchs, H. J. Kimble, and E. S. Polzik, "Unconditional quantum teleportation," *Sciences* **282**, p. 706, 1998.

4. W. P. Bowen, N. Treps, B. C. Buchler, R. Schnabel, T. C. Ralph, H.-A. Bachor, T. Symul, and P. K. Lam, "Experimental investigation of continuous variable quantum teleportation," *Phys. Rev. A* **67**, p. 032302, 2003.
5. K. McKenzie, D. A. Shaddock, D. E. McClelland, B. C. Buchler, and P. K. Lam, "Experimental demonstration of a squeezing-enhanced power-recycled michelson interferometer for gravitational wave detection," *Phys. Rev. Lett.* **88**, p. 231102, 2002.
6. J. Hald, J. L. Sorensen, C. Schori, and E. S. Polzik, "Spin squeezed atoms: A macroscopic entangled ensemble created by light," *Phys. Rev. Lett.* **83**, p. 1319, 1999.
7. K. Bencheikh, T. Symul, A. Jankovik, and J. A. Levenson, "Quantum key distribution with continuous variables," *J. of mod. opt.* **48**, p. 1903, 2001.
8. C. Fabre, "Squeezed states of light," *Phys. Reports* **219**, p. 215, 1992.
9. D. F. Walls and G. J. Millburn, *Quantum Optics*, Springer-Verlag, Berlin, 1994.
10. P. K. Lam, T. C. Ralph, B. C. Buchler, D. E. McClelland, H.-A. Bachor, and J. Gao, "Optimization and transfer of vacuum squeezing from an optical parametric oscillator," *J. Opt. B* **1**, p. 469, 1999.
11. J. W. Wu, P. K. Lam, M. B. Gray, and H.-A. Bachor, "Optical homodyne tomography of information carrying laser beams," *Optics Express* **3**, p. 154, 1998.
12. W. P. Bowen, R. Schnabel, P. K. Lam, and T. C. Ralph, "Experimental investigation of criteria for continuous variable entanglement," *Phys. Rev. Lett.* **90**, p. 043601, 2003.
13. N. Korolkova, G. Leuchs, R. Loudon, T. C. Ralph, and C. Silberhorn, "Polarization squeezing and continuous-variable polarization entanglement," *Phys. Rev. A* **65**, p. 052306, 2002.
14. W. P. Bowen, R. Schnabel, H.-A. Bachor, and P. K. Lam, "Polarization squeezing of continuous variable stokes parameters," *Phys. Rev. Lett.* **88**, p. 093601, 2002.
15. R. Schnabel, W. P. Bowen, N. Treps, T. C. Ralph, H.-A. Bachor, and P. K. Lam, "Stokes-operator-squeezed continuous-variable polarization states," *Phys. Rev. A* **67**, p. 012316, 2003.
16. C. Fabre, J. B. Fouet, and A. Maître, "Quantum limits in the measurement of very small displacements in optical images," *Optics Letters* **25**, p. 76, 2000.
17. N. Treps, U. Andersen, B. C. Buchler, P. K. Lam, A. Maître, H.-A. Bachor, and C. Fabre, "Surpassing the standard quantum limit for optical imaging using nonclassical multimode light," *Phys. Rev. Lett.* **88**, p. 203601, 2002.
18. P. Grangier, R. E. Slusher, B. Yurke, and A. LaPorta, "Squeezed-lightenhanced polarization interferometer," *Phys. Rev. Lett.* **59**, p. 2153, 1987.
19. W. P. Bowen, N. Treps, R. Schnabel, and P. K. Lam, "Experimental demonstration of continuous variable polarization entanglement," *Phys. Rev. Lett.* **89**, p. 253601, 2002.